

Hybrid Composites

DOI: 10.1002/anie.200601676

**Highly Reversible Lithium Storage in Spheroidal Carbon-Coated Silicon Nanocomposites as Anodes for Lithium-Ion Batteries\*\***

*See-How Ng, Jiazhao Wang, David Wexler, Konstantin Konstantinov, Zai-Ping Guo, and Hua-Kun Liu\**

Rechargeable lithium-ion batteries are key devices for today's information-based mobile society. One of the major challenges for designing electrode materials is to combine

[\*] S.-H. Ng, Dr. J. Wang, Dr. K. Konstantinov, Dr. Z.-P. Guo, Prof. H.-K. Liu  
 Institute for Superconducting & Electronic Materials  
 and ARC Centre of Excellence for Electromaterials Science  
 University of Wollongong  
 Wollongong, NSW 2522 (Australia)  
 Fax: (+ 61) 2-4221-5731  
 E-mail: hua\_liu@uow.edu.au  
 Homepage: <http://www.uow.edu.au/eng/research/isem/staff/hkliu.html>

Dr. D. Wexler  
 Faculty of Engineering  
 University of Wollongong  
 Wollongong, NSW 2522 (Australia)

[\*\*] Financial support provided by the Australian Research Council (ARC) through the ARC Centre of Excellence funding (CE0561616) is gratefully acknowledged. Moreover, the authors are grateful to Sau-Yen Chew at the University of Wollongong for experimental assistance. Finally, we also thank Dr. Tania Silver at the University of Wollongong for critical reading of the manuscript.



Supporting information for this article is available on the WWW under <http://www.angewandte.org> or from the author.

both high Li storage capacity and coulombic efficiency (that is, a high ratio of extractable Li to inserted Li).<sup>[1]</sup> Graphite and LiCoO<sub>2</sub>, both commonly used in Li-ion batteries, have high coulombic efficiencies (> 95 %) but rather low capacities (372 and 145 mA h g<sup>-1</sup>, respectively).<sup>[2,3]</sup> Many new materials, especially those that form alloys with lithium (for example, Sn, Sb, Si, and Ge),<sup>[4-7]</sup> have shown high capacity values, but generally suffer from low coulombic efficiencies (< 60 %) on the first few cycles. The low coulombic efficiencies can be attributed to a variety of shortcomings: for example, irreversible trapping of inserted Li ions by host materials, formation of the solid/electrolyte interface (SEI) layer, or the loss of electrical contact between the electrode material and the current collector. This low coulombic efficiency reduces the energy density of the Li-ion batteries significantly and poses a serious trade-off in battery technology.

Silicon-based negative electrodes for lithium-ion batteries have attracted great interest because of their high theoretical specific capacity of 4212 mA h g<sup>-1</sup>.<sup>[6]</sup> Of particular note are studies on nanostructured Si-based anodes, where it has been shown that a nanoparticle-based system improves the cycle lifetime.<sup>[8-10]</sup> Although nanocrystalline Si shows a high capacity for the first charge (ca. 2000 mA h g<sup>-1</sup>, depending on the compositions studied), it exhibits poor retention of capacity as a result of material degradation, which makes it unsuitable for practical commercial applications. This serious drawback, also known as the pulverization of silicon, is caused by the large change in volume during lithium-ion insertion/extraction. It is necessary to relieve such morphological changes to improve the cycling characteristics of this material. One possible solution to overcome this problem is by using composite materials, in which an electrochemically active phase is homogeneously dispersed within an electrochemically inactive matrix.<sup>[11,12]</sup> The inactive phase would accommodate the mechanical stresses/strains experienced by the active phase and maintain the structural integrity of the composite electrode during the alloying/de-alloying processes.

Recently, Holzapfel et al. obtained promising results for nanosized silicon/graphite composites prepared by a reductive decomposition of a silicon precursor. This composite shows a stable capacity of 1000 mA h g<sup>-1</sup>, with a Si content of 20 wt %.<sup>[13]</sup> However, the specific capacity has been limited by the small amount of Si in the composite material. Herein we report on carbon-coated Si nanocomposites produced by a spray-pyrolysis technique, which can reversibly store lithium with both a high capacity of 1489 mA h g<sup>-1</sup> and a high coulombic efficiency above 99.5 %, even after 20 cycles. The spray-pyrolysis method used in this study is instantaneous, versatile, inexpensive, industrially oriented, and can be operated over a large temperature range (150–1400 °C).<sup>[14]</sup>

Thermogravimetric analysis (TGA) of the carbon-coated Si nanocomposites carried out in air showed that the carbon content was 56 wt %, with the remaining 44 wt % estimated to be silicon. The TGA curves also show that Si will only be oxidized rapidly in air above 500 °C. Therefore, any spray-pyrolysis process conducted in air under 500 °C will not give rise to the presence of impurities such as SiO<sub>2</sub>. The X-ray-diffraction (XRD) pattern of the carbon-coated Si nano-

composites also shows only the Si peaks, thus confirming that there no bulk SiO<sub>2</sub> crystalline phase was formed during the spray-pyrolysis process at 400 °C in air. Moreover, no diffraction lines from crystalline carbon (graphite) were observed in the XRD pattern, thereby indicating the amorphous nature of the carbon in the nanocomposites.

Figure 1 shows TEM images of the carbon-coated Si nanocomposites. The size of the individual composite particles ranged from below 10 nm to approximately 100 nm

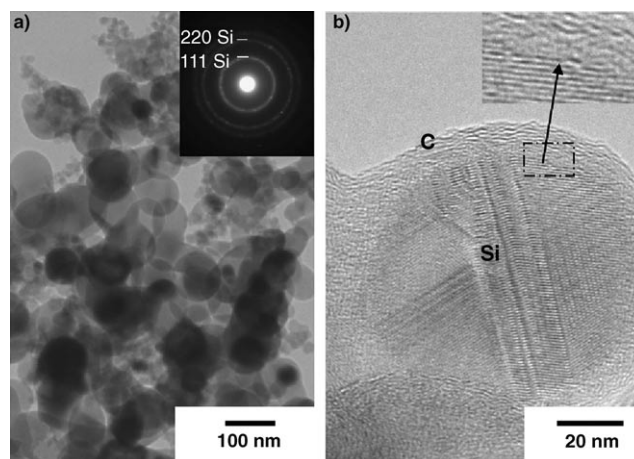


**Figure 1.** TEM images of spheroidal carbon-coated Si nanocomposites produced by spray pyrolysis in air: a) low-magnification image of a sample produced at 400 °C, with the indexed diffraction pattern (inset) confirming the presence of Si nanoparticles; b) high-resolution image showing the carbon-coated Si nanocomposite, with the inset showing the interface between a crystalline Si particle and the pyrolyzed carbon coating layer (ca. 10 nm thickness).

(Figure 1a). The fine dotted rings of the associated selected-area electron-diffraction pattern (inset in Figure 1a) correspond to nanocrystalline Si, although additional diffuse contrast within the diffraction rings may also indicate the presence of minor amounts of amorphous Si. Figure 1b clearly demonstrates the coexistence of two phases. The nanocrystalline Si particles were generally spheroidal, although some of the larger ones were faceted. The spheroidal Si particle in Figure 1b also contains microtwins and stacking faults. It is surrounded by an amorphous or semiamorphous carbon layer (C; ca. 10 nm in thickness). Contrast from carbon under high-magnification (see inset, Figure 1b) also indicated that the pyrolyzed carbon was predominately amorphous carbon although further high-resolution imaging experiments are required to confirm that no graphitic carbon is also present.

The electrochemical performance of the nanocrystalline Si precursor powder and the carbon-coated Si nanocomposite electrodes was systematically investigated. Figure 2 summarizes the discharge (lithiation) and charge (delithiation) capacity data for nanocrystalline Si and carbon-coated Si nanocomposite electrodes. The calculated capacities were solely based on the active material, either Si or carbon-coated Si-composite particles in the electrode. Even though the first discharge and charge capacities of the Si electrode (Fig-

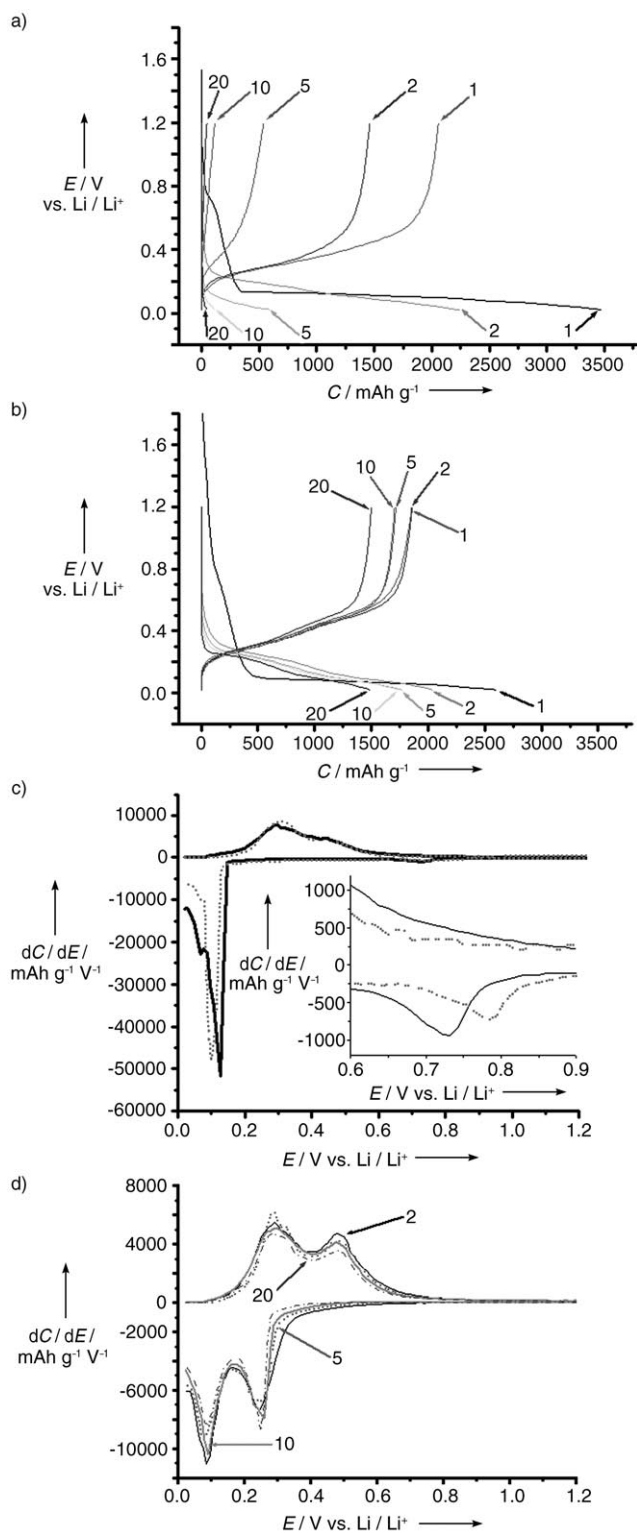


**Figure 2.** Charge–discharge plots of: a) a nanocrystalline Si electrode and b) a carbon-coated Si nanocomposite electrode with 44 wt% Si content (the numbers indicate the cycle number). c) First-cycle differential capacity plots of nanocrystalline Si (solid line) and carbon-coated Si nanocomposite (dotted line) electrodes (inset: enlarged plot of (c)). d) Differential capacity plots for the carbon-coated Si nanocomposite electrode (the numbers indicate the cycle number). Cycling took place between 0.02 V and 1.20 V versus  $Li/Li^+$  at a cycling rate of  $100\ mA\ g^{-1}$ .  $C$  = capacity,  $E$  = cell potential,  $dC/dE$  = differential capacity.

ure 2a) were  $3474\ mA\ h\ g^{-1}$  and  $2058\ mA\ h\ g^{-1}$ , respectively, further cycling led to a rapid decay of the capacity to  $47\ mA\ h\ g^{-1}$  after 20 cycles. Note that the initial ratio of the irreversible capacity was 41%. This result is consistent with those reported by Yang et al. for a nanocrystalline Si ( $< 100\ nm$ ) electrode.<sup>[15]</sup> This result indicates that a reduction in the particle size cannot prevent aggregation of Si on the micrometer scale. In contrast, the first discharge and charge capacities of the amorphous carbon-coated Si nanocomposite electrode (Figure 2b) were  $2600\ mA\ h\ g^{-1}$  and  $1857\ mA\ h\ g^{-1}$ , respectively. The initial ratio of the irreversible capacity was 29%, which is 12% lower than that of the Si particles only. In addition, the amorphous carbon-coated Si nanocomposite electrodes exhibited an excellent cycling properties, retaining a specific capacity of approximately  $1489\ mA\ h\ g^{-1}$  after 20 cycles.

The differential capacity curves of the carbon-coated Si nanocomposite electrode exhibited essentially the same peak features as the Si electrode below 0.3 V (Figure 2c). However, the first cathodic peak was shifted from 0.12 V (Si) to 0.09 V (Si-C). This effect arises because the solid/electrolyte interface is different for both cases (namely, Si/electrolyte and carbon/electrolyte, respectively). Therefore, the surface kinetics will be different, thus resulting in the shifted peaks that are seen in the differential capacity curves.<sup>[16]</sup> Furthermore, a clear irreversible reaction corresponding to formation of the Si/electrolyte interface near 0.73 V was not found for the carbon-coated Si nanocomposite electrode, but instead formation of a carbon/electrolyte interface layer was observed near 0.78 V for the carbon-coated Si nanocomposite electrode. This phenomenon could be attributed to the masking effects from the spray-pyrolyzed carbon layer.<sup>[17]</sup> It was also clearly demonstrated (Figure 2d) that the carbon-coated Si nanocomposite electrode maintained high activity and reversibility, even after 20 cycles. The improved performance could be attributed to the amorphous carbon coating with high electronic conductivity, which not only buffered the large changes in the volume during the cycling process but also avoided possible agglomeration of the uniformly distributed silicon particles.<sup>[15–17]</sup>

Figure 3 shows the cycling behavior of the carbon-coated Si nanocomposite electrode. An initial lithiation capacity of

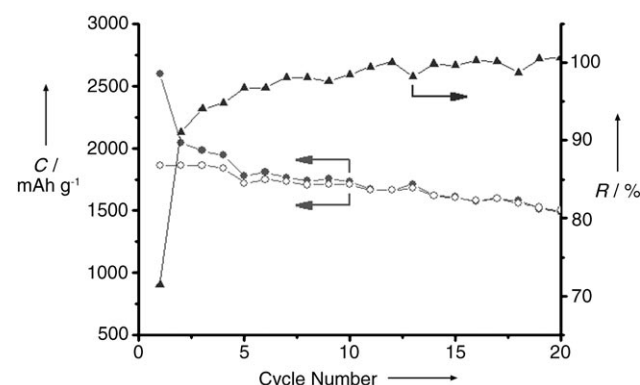


**Figure 3.** Cycling behavior of the carbon-coated Si nanocomposite electrode with 44 wt% Si content, cycled between 0.02 V and 1.20 V at a cycling rate of  $100\ mA\ g^{-1}$ . ● =  $Li^+$  insertion, ○ =  $Li^+$  extraction, ▲ = coulombic efficiency;  $C$  = capacity,  $R$  = coulombic efficiency.

2600 mA h g<sup>-1</sup> and a delithiation capacity of 1857 mA h g<sup>-1</sup> for the active materials (44% Si + 56% C) was obtained by using a nonrestricted cycling procedure. This low initial coulombic efficiency (71.4%) of the carbon-coated Si nanocomposites is mainly a consequence of the large insertion capacity (ca. 700 mA h g<sup>-1</sup>) contributed by the amorphous carbon content. Subsequently, the carbon-coated Si nanocomposite electrode retained a specific capacity of about 1489 mA h g<sup>-1</sup> after 20 cycles. By subtracting the capacity of the spray-pyrolyzed carbon from that of citric acid (ca. 100 mA h g<sup>-1</sup> after 20 cycles), which was measured separately, the discharge capacity delivered by the Si component (44 wt%) was estimated to be approximately 1433 mA h. Therefore, the specific capacity of Si in the composite electrode was calculated to be 3257 mA h g<sup>-1</sup>, which amounts to an impressive 77% of the theoretical value (4212 mA h g<sup>-1</sup>). This result shows the beneficial effect of the carbon coating on the enhanced dimensional stability of the Si particles during the Li alloying/de-alloying process, which makes possible further significant improvement to the electric conductivity of the composites.<sup>[15-17]</sup>

In conclusion, spheroidal carbon-coated Si nanocomposite, prepared by a spray-pyrolysis method in air, is a promising candidate for use as an anode material in lithium-ion batteries, as it has excellent retention of specific capacity, high coulombic efficiency, and low cost (because of the abundance of both Si and carbon sources).

### Experimental Section

Citric acid (C<sub>6</sub>H<sub>8</sub>O<sub>7</sub>, Sigma Aldrich) was dissolved in absolute ethanol (200 mL, 99.99 wt %, Merck) with continuous stirring. Nanocrystalline Si powder (<100 nm, Nanostructured and Amorphous Materials Inc.) was then mixed into the initial citric acid/ethanol solution (1:10 Si: citric acid w/w) by ultrasonication for 90 mins. The nanocomposite material was obtained in situ by spray-pyrolyzing the Si/citric acid/ethanol suspensions at 400°C with a flow rate of 4 mL min<sup>-1</sup> into a vertical-type spray-pyrolysis reactor. The spray-pyrolysis reaction of Si in citric acid/ethanol solution can be expressed as Equation (1).



Accurate carbon contents in the spray-pyrolyzed composites were determined by TGA and differential thermal analyses on Setaram 92 equipment. The sprayed powders were characterized by XRD using a Philips PW1730 diffractometer with Cu<sub>Kα</sub> radiation and a graphite monochromator. TEM investigations were performed using a JEOL 2011 200 KeV analytical electron microscope. TEM samples were prepared by deposition of ground particles onto lacey carbon support films.

The anode was prepared by mixing nanocrystalline Si, spray-pyrolyzed carbon-coated Si nanocomposites, or spray-pyrolyzed carbon from citric acid as active materials with 10 wt% carbon black (Super P, MMM, Belgium) and 10 wt% polyvinylidene fluoride binder in *N*-methyl-2-pyrrolidinone solvent to form a homogeneous slurry, which was then spread onto a copper foil. The coated electrodes (average thickness of ca. 50 μm) were dried in a vacuum oven at 110°C for 24 h and then pressed. Electrochemical measurements were carried out using coin-type cells. CR 2032 coin-type cells were assembled in an argon-filled glove box (Mbraun, Unilab, Germany) by stacking a porous polypropylene separator containing liquid electrolyte between the composite electrodes and a lithium-foil counter electrode. The electrolyte used was 1M LiPF<sub>6</sub> in a 50:50 (v/v)

mixture of ethylene carbonate and dimethyl carbonate obtained from MERCK KGaA, Germany. The cells were galvanostatically charged and discharged in the range of 0.02–1.20 V at a constant current density of 100 mA g<sup>-1</sup>.

Received: April 28, 2006

Revised: July 31, 2006

Published online: September 26, 2006

**Keywords:** batteries · carbon · electrochemistry · lithium · silicon

- [1] J.-M. Tarascon, M. Armand, *Nature* **2001**, *414*, 359.
- [2] J. R. Dahn, T. Zheng, Y. Liu, J. S. Xue, *Science* **1995**, *270*, 590.
- [3] M. Winter, J. O. Besenhard, M. E. Spahr, P. Novak, *Adv. Mater.* **1998**, *10*, 725.
- [4] Y. Idota, T. Kubota, A. Matsufuji, Y. Maekawa, T. Miyasaka, *Science* **1997**, *276*, 1395.
- [5] H. Li, L. Shi, W. Lu, X. Huang, L. Chen, *J. Electrochem. Soc.* **2001**, *148*, A915.
- [6] B. A. Boukamp, G. C. Lesh, R. A. Huggins, *J. Electrochem. Soc.* **1981**, *128*, 725.
- [7] N. Pereira, M. Balasubramanian, L. Dupont, J. McBreen, L. C. Klein, G. G. Amatucci, *J. Electrochem. Soc.* **2003**, *150*, A1118.
- [8] J. Yang, B. F. Wang, K. Wang, Y. Liu, J. Y. Xie, Z. S. Wen, *Electrochem. Solid-State Lett.* **2003**, *6*, A154.
- [9] C. S. Wang, G. T. Wu, X. B. Zhang, Z. F. Qi, W. Z. Li, *J. Electrochem. Soc.* **1998**, *145*, 2751.
- [10] A. M. Wilson, J. R. Dahn, *J. Electrochem. Soc.* **1995**, *142*, 326.
- [11] O. Mao, R. L. Turner, I. A. Courtney, B. D. Fredericksen, M. I. Buckett, L. J. Krause, J. R. Dahn, *Electrochem. Solid-State Lett.* **1999**, *2*, 3.
- [12] I. S. Kim, P. N. Kumta, G. E. Blomgren, *Electrochem. Solid-State Lett.* **2000**, *3*, 493.
- [13] M. Holzappel, H. Buqa, W. Scheifele, P. Novak, F.-M. Petrat, *Chem. Commun.* **2005**, *12*, 1566.
- [14] S. H. Ng, J. Wang, K. Konstantinov, D. Wexler, J. Chen, H. K. Liu, *J. Electrochem. Soc.* **2006**, *153*, A787.
- [15] X. Yang, Z. Wen, X. Zhu, S. Huang, *Electrochem. Solid-State Lett.* **2005**, *8*, A481.
- [16] N. Dimov, S. Kugino, M. Yoshio, *Electrochim. Acta* **2003**, *48*, 1579.
- [17] Y. Liu, T. Matsumura, N. Imanishi, A. Hirano, T. Ichikawa, Y. Takeda, *Electrochem. Solid-State Lett.* **2005**, *8*, A599.